Supplement of Atmos. Chem. Phys., 25, 16387–16399, 2025 https://doi.org/10.5194/acp-25-16387-2025-supplement © Author(s) 2025. CC BY 4.0 License.





## Supplement of

## Underestimation of atmospheric oxidized mercury at a mountaintop site by the GEOS-Chem chemical transport model

Tyler R. Elgiar et al.

Correspondence to: Seth N. Lyman (seth.lyman@usu.edu)

The copyright of individual parts of the supplement might differ from the article licence.

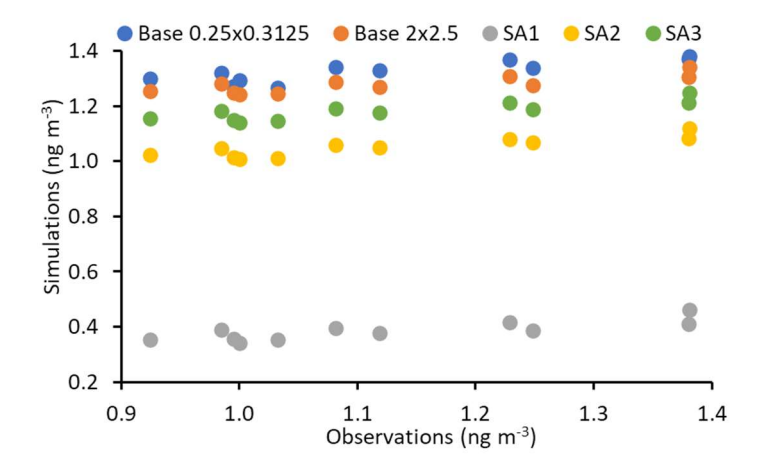


Figure S1. Observed versus simulated Hg<sup>0</sup>.

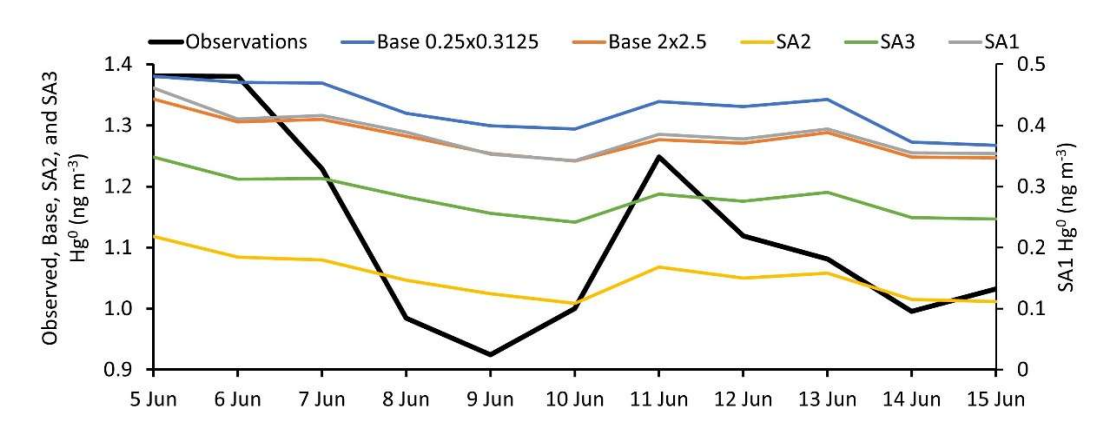


Figure S2. Observed and simulated daily average  ${\rm Hg^0}$  from 5 to 15 June 2021.

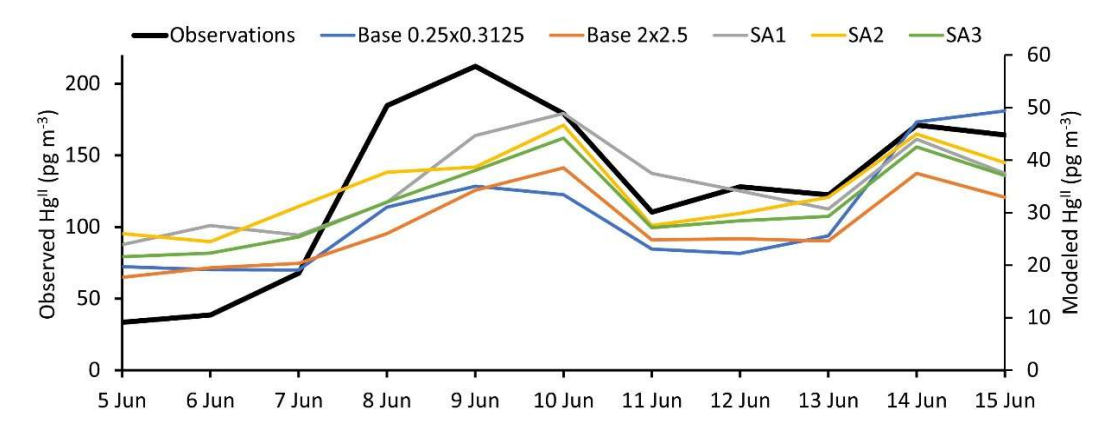


Figure S3. Observed and simulated daily average HgII from 5 to 15 June 2021.

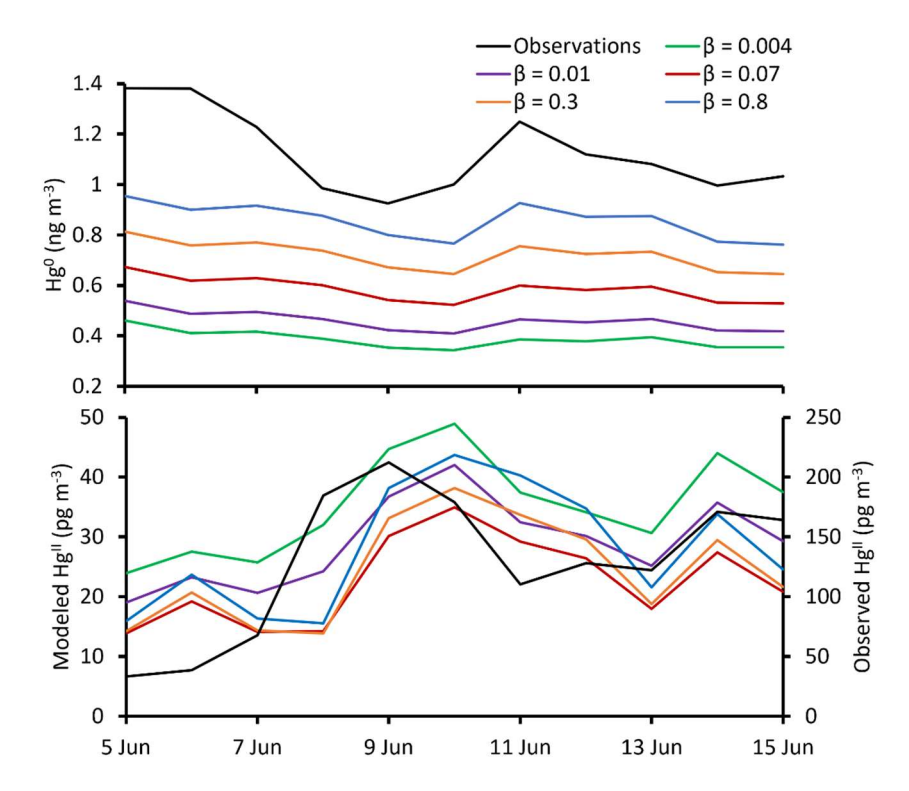


Figure S4. Observed  $Hg^0$  and  $Hg^{II}$ , and model sensitivity analyses using the same  $Hg^0 + Br$  chemistry from SA1, but with the photoreduction rate of organic particulate  $Hg^{II}$  increased to allow for increased  $Hg^0$ . The photoreduction rate scales to the  $NO_2$  photolysis rate using a scaling factor  $\beta$ , and the default value in the model version used was 0.004. Modeled and observed  $Hg^{II}$  are shown on different y axes.

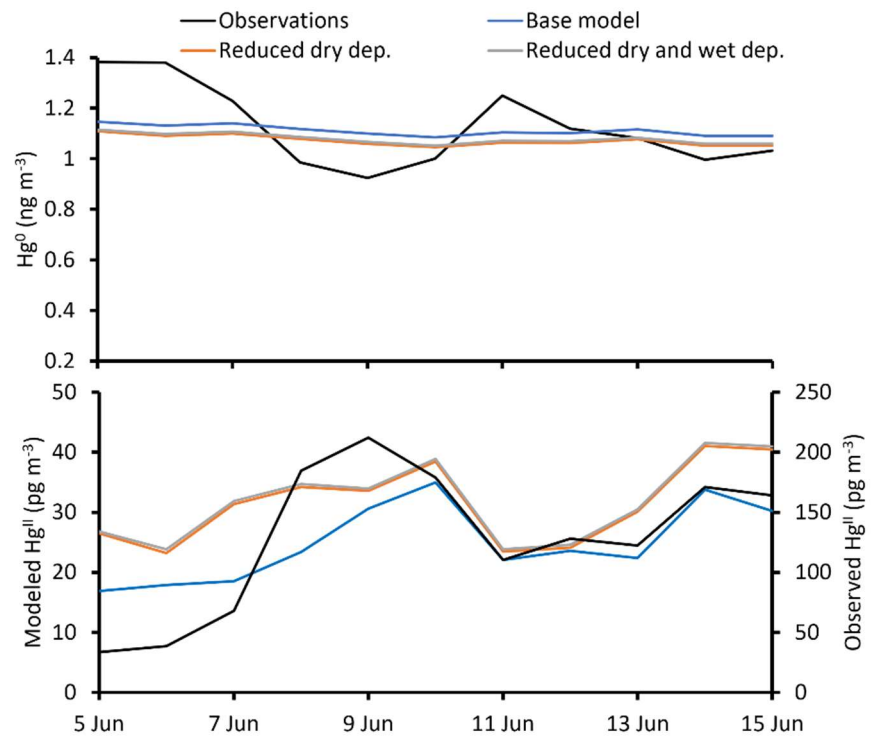


Figure S5. Observed Hg $^0$  and Hg $^{II}$ , and model sensitivity analyses using GEOS-Chem version 14.1. Base model is the model output with default settings for version 14.1. Reduced dry deposition shows model output with DD\_Hstar reduced from  $1.0 \times 10^{14}$  to  $1.0 \times 10^{5}$ . Reduced dry and wet deposition shows model output with Henry\_K0 reduced from  $1.40 \times 10^{6}$  to  $1.40 \times 10^{4}$ .

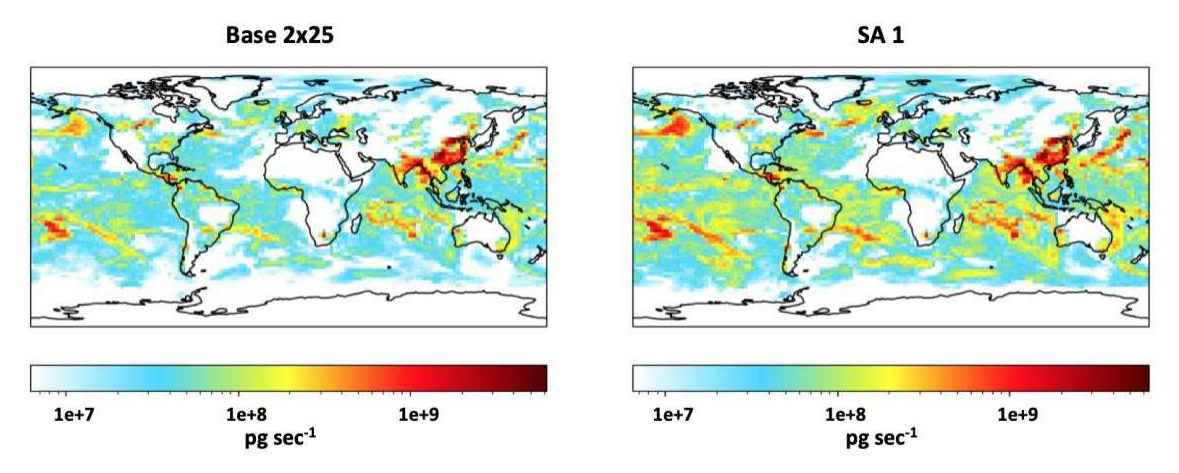


Figure S6. Average wet loss in large scale precipitation events for the Base 2x25 and SA1 simulations on 9 June 2021.

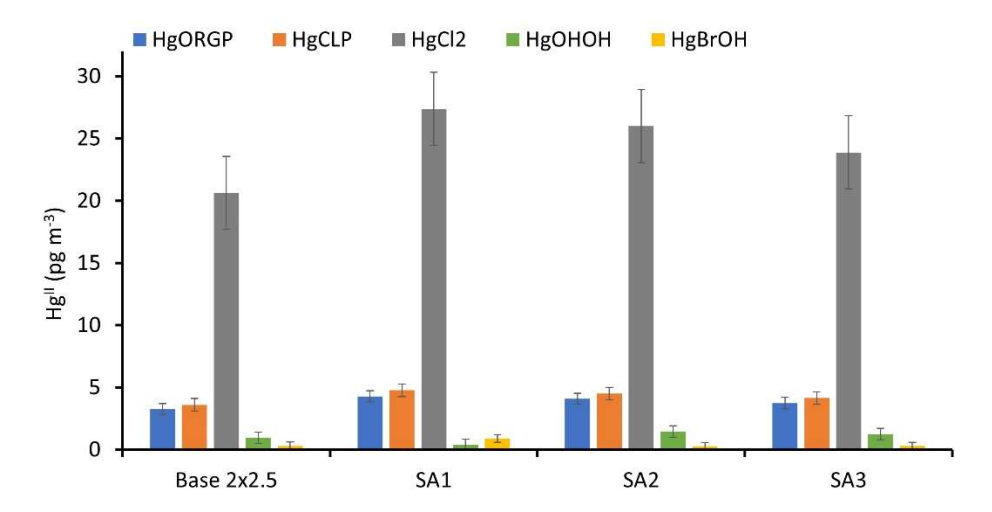


Figure S7. Dominant average modeled Hg<sup>II</sup> species for the period of 7 to 11 June 2021. HgORGP represents the fraction of Hg present in organic aerosols. HgCLP represents the fraction of Hg present in chloride salts on sea-salt aerosols. Bars show averages, and whiskers show standard deviations.

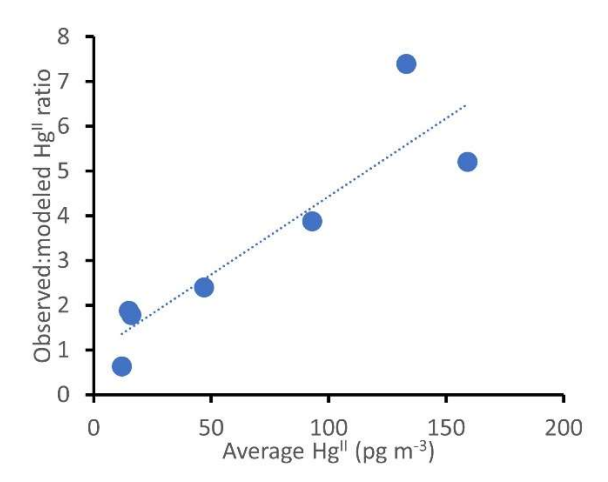


Figure S8. Average  $Hg^{II}$  observed in this study and from Gustin et al. (2023), as shown in Table 4, versus the observed:modeled  $Hg^{II}$  ratio, also as shown in Table 4.

Table S1. Model performance for Hg<sup>II</sup> and Hg<sup>0</sup> using statistics recommended by Chang and Hannah (2004). Calculations performed were the fraction of predictions within two factors of observations (FAC2), fractional mean bias (FB), geometric mean bias (MG), normalized mean square error (NMSE), and geometric variance (VG). A value of 0 for FB and NMSE represents a perfect model, larger values indicate under-prediction. A value of 1 for FAC2, MG, and VG represents a perfect model. Larger values for MG and VG indicate under-prediction.

Hg <sup>II</sup>	Simulation	FAC2	FB	MG	NMSE	VG
	Base 0.25x0.3125	0.09	1.25	3.96	3.23	7.87
	Base 2x2.5	0.18	1.30	4.20	3.68	9.04
	SA1	0.18	1.14	3.22	2.52	4.78
	SA2	0.18	1.15	3.27	2.61	5.00
	SA3	0.18	1.21	3.59	2.96	6.10
	Base 0.25x0.3125	1	-0.16	0.84	0.04	1.04

$Hg^0$	Base 2x2.5	1	-0.13	0.87	0.03	1.03
	SA1	0	0.98	2.90	1.30	3.14
	SA2	1	0.07	1.06	0.02	1.01
	SA3	1	-0.05	0.94	0.01	1.02